Synthesis and biological evaluation of combretastatin-amidobenzothiazole conjugates as potential anticancer agents

ARTICLE *in* EUROPEAN JOURNAL OF MEDICINAL CHEMISTRY · AUGUST 2012

Impact Factor: 3.45 · DOI: 10.1016/j.ejmech.2012.08.021 · Source: PubMed

11 AUTHORS, INCLUDING:

Ahmed Kamal
Indian Institute of Chemical Technology
489 PUBLICATIONS **6,097** CITATIONS
SEE PROFILE

Janaki Ramaiah
Indian Institute of Chemical Technology
61 PUBLICATIONS **651** CITATIONS
SEE PROFILE

Chandan Kishor
18 PUBLICATIONS **174** CITATIONS
SEE PROFILE

Anthony Addlagatta
Indian Institute of Chemical Technology
84 PUBLICATIONS **1,047** CITATIONS
SEE PROFILE

European Journal of Medicinal Chemistry 56 (2012) 166–178

Contents lists available at SciVerse ScienceDirect

European Journal of Medicinal Chemistry

journal homepage: http://www.elsevier.com/locate/ejmech

Original article

Synthesis and biological evaluation of combretastatin-amidobenzothiazole conjugates as potential anticancer agents

Ahmed Kamal [a,*], Adla Mallareddy [a], M. Janaki Ramaiah [b], S.N.C.V.L. Pushpavalli [b], Paidakula Suresh [a], Chandan Kishor [b], J.N.S.R.C. Murty [a], N. Sankara Rao [a], Sowjanya Ghosh [a], Anthony Addlagatta [b,*], Manika Pal-Bhadra [b,*]

[a] Division of Organic Chemistry, CSIR-Indian Institute of Chemical Technology, Tarnaka, Hyderabad 500 607, India
[b] Centre for Chemical Biology, CSIR-Indian Institute of Chemical Technology, Tarnaka, Hyderabad 500 607, India

ARTICLE INFO

Article history:
Received 29 March 2012
Received in revised form
6 July 2012
Accepted 15 August 2012
Available online 23 August 2012

Keywords:
CA-4
Cell cycle
Anticancer activity
ERK
Tubulin
Molecular modeling

ABSTRACT

A series of combretastatin-amidobenzothiazole conjugates have been synthesized and evaluated for their anticancer activity. All these compounds exhibited significant anticancer activity and the most potent compound (**11a**) showed GI_{50} values ranging 0.019–11 μM. Biological studies such as cell cycle distribution, effect on tubulin polymerization and effect on ERK signalling pathway have been examined in MCF-7 cell line. FACS analysis revealed that these compounds induced cell cycle arrest at G2/M phase. Compound **11a** showed significant effect on tubulin polymerization and affected the ERK signalling pathway that result in the decreased levels of ERK1/2, p-ERK and c-Jun proteins. Docking experiments have shown that the active molecules interact and bind well in the ATP binding pocket of ERK protein.

1. Introduction

Mitogen-activated protein kinases (MAPKs) transduce extracellular stimuli from the cell surface to the nucleus, leading to alterations in gene expression and cell functions. To date, three major subfamilies of MAPKs have been identified: c-Jun N-terminal kinases/stress-activated protein kinases (JNK/SAPKs), extracellular signal-regulated kinases (ERK1/2 or p42/44 MAPK) and p38 MAPK [1]. The extracellular signal-regulated kinase (ERK) signalling pathway controls proliferation, differentiation and cell survival processes [2–4]. ERK1/2 is primarily activated (phosphorylated) by mitogens (MEK1/2) and growth factors and plays a key role in transmission of proliferative signals in mammalian cells. Activated ERK1/2 then phosphorylate serine/threonine residues of more than 50 downstream cytosolic and nuclear substrates, leading to alterations in gene expression profiles that are implicated in proliferation, differentiation and cell survival [2–4]. Tyrosine kinase mediated signalling, which exists in cancers as well as other proliferative disorders cause abnormal phosphorylation of ERK and MAPK [5,6]. The ERK signalling as well as c-Jun are known to be the key molecules that regulate breast cancer cell migration [7]. This prompted us to design and synthesize molecules based on combretastatin scaffold that are likely to mediate the above pathways and could generate agents useful towards the treatment of particularly breast cancers.

Combretastatin A-4 (**2**) which is isolated from the bark of the South African Cape Bush willow (*Combretum caffrum*), exhibits potent anticancer activity against a number of human cancer cell lines [8] (Fig. 1). It acts as a microtubule destabilizing agent by binding to the tubulin at the site similar to that of colchicine (**1**) [9]. A water-soluble prodrug, combretastatin A-4-phosphate (**3**) is now in clinical trials for thyroid cancer [10–12] and in patients with advanced cancer [13]. Interestingly, the *cis* form of **2** alone is biologically active, with the trans form showing little or no activity [14]. Various structural modifications to CA-4 have been reported including variation of the A- and B-ring substituents [15–17]. It has been observed that most of the modifications of the B-ring result in decreased bioactivity; however, substitution of the 3′-OH with an amino group results in the enhancement of bioactivity and better water solubility [18]. This amino derivative of CA-4 (**4**) is

* Corresponding authors. Tel.: +91 40 27193157; fax: +91 40 27193189.
E-mail addresses: ahmedkamal@iict.res.in (A. Kamal), manika@iict.res.in (M. Pal-Bhadra).

0223-5234/$ – see front matter © 2012 Elsevier Masson SAS. All rights reserved.
http://dx.doi.org/10.1016/j.ejmech.2012.08.021

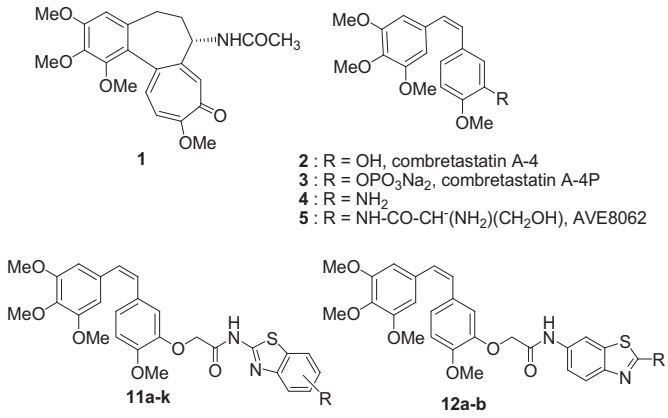

Fig. 1. Chemical structures of colchicine (**1**), combretastatins (**2**–**5**) and combretastatin-benzothiazole conjugates (**11a**–**k** and **12a**–**b**).

also in clinical trials as a water-soluble amino acid prodrug (**5**) [19]. The 3,4,5-trimethoxy substituted pattern in ring A, resembling the trimethoxyaryl ring of colchicine, is considered optimal for the bioactivity of CA-4 [20]. Many conformationally restricted analogues of CA-4 have been reported, wherein the *cis*-double bond has been replaced by a heterocyclic rigid ring scaffold structure. Being a potent inhibitor of colchicine binding, CA-4 has also shown to inhibit the growth and development of blood vessels [21–24]. It is also demonstrated that mitogen-activated protein kinases are involved in the cytotoxicity of CA-4 [25]. Benzothiazoles constitute an important scaffold of drugs, possessing several pharmacological functions [26,27], and exhibit potent and intriguing antitumor properties [28–30]. It is reported that some of the 6-substituted 2-phenylbenzothiazole derivatives have shown good anticancer activity [31,32]. Apart from this, some benzothiazole derivatives as sub structure have shown to inhibit ERK phosphorylation [33].

It was reported [25] that the cytotoxicity of CA-4 also caused by affecting MAPK family of proteins and benzothiazole derivatives exerts inhibitory activity on ERK phosphorylation [33]. The encouraging anticancer profile of combretastatin and benzothiazole scaffolds and their effect on MAP kinases led us to synthesize new conjugates of combretastatin. Herein we report the synthesis of combretastatin-benzothiazole conjugates fused with amide bond and evaluation of their anticancer potential. The synthesized compounds were also evaluated for their effect on tubulin polymerization and ERK signalling. Moreover, the ERK inhibition exhibited by selective compounds is rationalized by molecular docking investigations.

2. Results and discussion

2.1. Chemistry

The synthesis of new combretastatin-amidobenzothiazole conjugates is shown in Scheme 1 from CA-4. The synthesis of natural product CA-4 is shown in Scheme 1 and compound **7** was prepared according to the reported procedure [34,35]. Compound **7** on Wittig reaction conditions at 0 °C with trimethoxybenzaldehyde gives geometrical isomers (**8a** and **8b**) in the ratio of 3:2. The *cis* and *trans* isomers were separated by flash column chromatography by using 5% ethyl acetate in hexane as eluent. The conversion of *trans* isomer to *cis* isomer was achieved in good yield under photochemical conditions [34]. The *cis* isomer **8a** upon treatment with TBAF undergoes deprotection to afford the compound **2**, as shown in Scheme 1. CA-4 upon etherification with α-bromoethyl acetate in the presence of K_2CO_3 gives ester **9** followed by its hydrolysis with $LiOH.H_2O$ to afford the acid **10**. The synthesis of amidobenzothiazole analogues of combretastatin A-4 (**11a**–**k**) was achieved by the formation of amide bond between this acid (**10**) and a variety of substituted 2-aminobenzothiazoles by using EDCI/HOBt. Similarly, other analogues (**12a,b**) were synthesized using 6-aminobenzothiazoles as shown in Scheme 1.

2.2. Biological evaluation

2.2.1. Anticancer activity

The synthesized compounds were first evaluated for their anticancer activity against selected human cancer cell lines of lung, colon, leukaemia, CNS, breast, liver and prostate by using sulforhodamine B (SRB) method [36]. The results are expressed in % of growth inhibition values at concentration of 10 μM as shown in Table 1. The compounds exhibiting % of growth inhibition values >50 are considered to be active on the respective cell lines. It is observed that all the compounds exhibit significant activity with >50% of growth inhibition values. Amongst the nine compounds synthesized, six compounds were evaluated under the 60 cell line screening program by the National Cancer Institute (NCI), Bethesda, USA. After preliminary screening on the tumour cell lines, these compounds were tested for five dose concentration on a panel of 59 human tumour cell lines derived from nine different cancer types: leukemia, lung, colon, CNS, melanoma, ovarian, renal, prostate and breast. The results expressed as GI_{50} values [37] for the test compounds are illustrated in Table 2. All the compounds exhibited potential anticancer activity with GI_{50} values ranging from 0.019 to 18.6 μM. It is observed that the anticancer activity for these combretastatin congeners is dependent on the nature of substituent present on the benzothiazole ring system. Amongst all the compounds tested for five dose studies, compound **11a** which does not have a substituent on the benzene ring of benzothiazole showed potent anticancer activity as compared to the compounds that had different substituent on 6-position of benzothiazole ring. The anticancer activity (GI_{50}) of this potential compound **11a** was in the range of 0.019–11 μM. This compound exhibited remarkable growth inhibition (19 and 51 nM) towards MDA-MB-435 and MCF-7 cell lines, respectively. This most active compound **11a** showed nano molar level activity against twenty three cancer cell lines and sub-micro molar level activity in twenty two cell lines. The other compounds showed micro molar level activity except one cell line in case of **11b** and **12b** which showed sub-micro molar activity against MDA-MB-435 and MCF-7 cell lines, respectively. It is observed that compound **11b** with 6-fluorobenzothiazole moiety showed better anticancer activity (0.33 μM) against MDA-MB-435 melanoma human cancer cell line in comparison to the other compounds (**11e**–**g**) that have methoxy, trifluoromethoxy and trifluoromethyl substitutions on the benzothiazole moiety. The analogue **12b** that has 6-amidobenzothiazole group also exhibited promising anticancer activity (GI_{50}, 0.74–9.41 μM) and showed activity of 0.74 μM against MCF-7 cell line.

Significant anticancer activity showed by these compounds prompted us to evaluate the cell viability on MCF-7 cells. The MCF-7 cells were treated with compounds **11a**, **11b**, **11e**, **11f**, **11g**, **11h**, **11i**, **11j**, **11k**, **12b** and starting materials CA-4 and 2-aminobenzothiazole (BT) at 4 μM concentration for 24 h. The viable cells after compound treatment were assayed by MTT based cell viability studies. It was observed that the compounds **11a** and **11b** showed slightly better activity as compared to other compounds (Fig. 2).

2.2.2. Effect of compounds on cell cycle

It is well established that CA-4 shows G2/M arrest whereas benzothiazoles cause G1 cell cycle arrest [38]. In order to

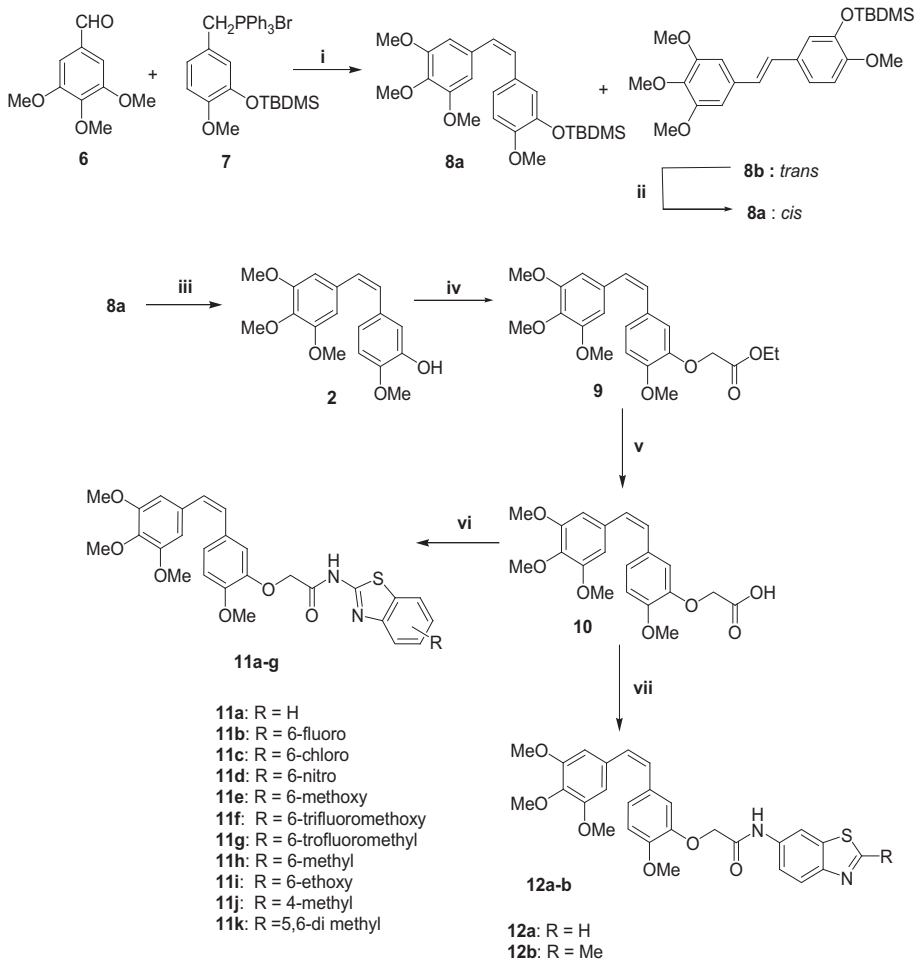

Scheme 1. Reagents and conditions: (i) NaH, CH_2Cl_2, 0 °C, 14 h, 40%; (ii) EtOH, sunlight, 6–7 h, 72%; (iii) TBAF, THF, 0 °C, 20 min, 79%; (iv) 2-bromoethyl acetate, K_2CO_3, DMF, 24 h, 94%; (v) LiOH, THF, H_2O, 12 h, 80%; (vi) 2-aminobenzothiazoles, EDCI, HOBt, CH_2Cl_2, 24 h, 83–93%; (vi) 6-aminobenzothiazoles, EDCI, HOBt, CH_2Cl_2 24 h, 88–89%.

Table 1
Percentage of growth inhibition[a] for selected cancer cell lines by combretastatin–benzothiazole conjugates at 10 μM concentration.

Comp	A549[b]	Colo205[c]	THP-1[d]	IMR32[e]	MCF-7[f]	Hep-2[g]	PC-3[h]
11a	44	60	na	91	72	na	44
11b	44	50	54	77	56	64	32
11c	na[j]	17	70	51	21	47	41
11d	50	46	80	88	69	na	47
11e	45	56	72	73	53	71	33
11f	40	41	66	44	59	78	34
11g	30	25	29	23	62	76	42
11h	37	33	27	na	57	44	22
11i	27	45	37	54	35	49	37
11j	na	24	19	34	29	na	24
11k	41	51	76	55	68	23	36
12a	na	11	41	46	19	20	58
12b	na	17	59	62	52	40	61
ADR[i]	52	26	83	73	45	56	75
CA-4	55	63	87	89	71	64	76

[a] Inhibition of cell proliferation after an incubation time of 48 h.
[b] Lung cancer cell line.
[c] Colon cancer cell line.
[d] Leukemia cancer cell line.
[e] Neuro cancer cell line.
[f] Breast cancer cell line.
[g] Liver cancer cell line.
[h] Prostate cancer cell line.
[i] Adriamycin.
[j] Not active.

Table 2
Anticancer activity (GI_{50})[a] of compounds **11a**, **11b**, **11e**, **11f**, **11g**, **12b** and **2**[b] against the NCI human cancer cell lines.

Panel/cell line	**11a**[c]	**11b**[d]	**11e**[e]	**11f**[f]	**11g**[g]	**12b**[h]	**2**
Leukemia							
CCRF-CEM	0.078	3.70	3.87	4.12	4.27	3.41	0.002
K-562	0.042	3.62	3.6	3.43	3.3	2.19	0.002
MOLT-4	0.34	3.07	3.87	4.21	3.75	2.11	0.003
RPMI-8226	0.15	6.36	5.43	5.83	5.48	1.98	0.003
SR	0.037	2.19	3.69	3.55	3.35	2.93	0.003
Non-small cell lung							
A549/ATCC	0.34	5.99	5.19	6	4.46	2.1	0.015
EKVX	0.038	5.72	5.11	7.89	6.25	4.05	0.079
HOP-62	nt[i]	5.70	23	7.09	5.22	3.09	0.002
HOP-92	0.039	5.73	6.28	2.74	2.88	2.38	0.002
NCI-H226	0.27	5.60	4.51	4.3	3.17	2.75	0.003
NCI-H23	0.11	4.26	3.91	4.39	3.9	2.53	0.003
NCI-H322M	nt	na[j]	na	na	5.38	6.74	0.003
NCI-H460	0.052	4.36	3.73	4.11	3.55	3.36	0.007
NCI-H522	0.079	2.92	3.09	3.16	2.89	2.28	0.001
Colon							
COLO-205	2.83	7.78	3.89	43.3	17.1	4.4	0.1
HCC-2998	0.37	na	7.34	17.1	4.23	6.9	0.063
HCT-116	0.046	4.48	3.7	3.92	3.29	3.57	0.003
HCT-15	0.048	8.19	2.89	3.23	3.24	2.8	0.003
HT29	3.16	9.63	3.34	na	14.9	3.31	0.1
KM12	0.058	4.78	3.12	4.48	3.14	3.79	0.005
SW-620	nt	na	5.1	5.65	4.65	4.7	0.003

Table 2 (*continued*)

Panel/cell line	11a[c]	11b[d]	11e[e]	11f[f]	11g[g]	12b[h]	2
CNS							
SF-268	0.18	7.23	4.31	6.01	3.85	3.61	0.006
SF-295	0.22	4.29	1.84	3.7	3.36	2.45	0.003
SF-539	0.045	4.51	2.84	2.28	2.66	2.56	0.002
SNB-19	nt	na	6.3	7.08	5.03	3.89	0.003
SNB-75	0.046	4.39	1.91	1.56	1.58	1.55	0.007
U251	0.048	4.33	4	3.37	3.67	3.59	0.007
Melanoma							
LOX IMVI	0.067	3.23	4.17	4.77	4.01	2.64	0.003
MALME-3M	1.99	5.22	na	nt	na	2.84	0.019
M14	0.072	6.82	4.33	4.36	3.58	3.38	0.002
MDA-MB-435	0.019	0.33	1.16	1.93	1.84	2.13	0.001
SK-MEL-2	0.18	8.46	4.07	3.29	3.98	3.15	0.003
SK-MEL-28	nt	na	4.41	4.57	3	3.22	0.007
SK-MEL-5	0.036	1.76	2.68	3.26	2.84	1.97	0.003
UACC-257	11	8.69	63	na	40	1.73	0.003
UACC-62	0.063	4.05	5.93	5.11	3.9	2.19	0.005
Ovarian							
IGROV1	0.21	4.17	7	5.64	4.48	3.72	0.015
OVCAR-3	0.043	9.99	2.17	3.37	2.11	6.32	0.001
OVCAR-4	0.37	7.30	5.31	5.34	4.66	2.64	0.015
OVCAR-5	nt	na	5.89	3.12	5.98	6.69	0.1
OVCAR-8	0.25	7.15	5.28	5	3.86	2.12	0.003
NCI/ADR-RES	0.033	2.55	2.3	2.7	2.12	2.36	0.001
SK-OV-3	0.34	8	4.69	8.42	3.29	5.27	0.063
Renal							
786-0	7.3	7.12	7.52	na	6.96	7.55	0.1
A498	0.36	6.25	3.5	3.61	2.81	4.18	0.006
ACHN	0.093	3.33	7.77	8.31	4.82	3.12	0.006
CAKI-1	0.41	2.78	3.2	4.6	3.1	2.19	0.025
RXF 393	0.05	6.29	2.5	2.65	2.27	5.06	0.002
SN12C	0.37	4.61	5.75	6.42	4.43	3.53	0.006
TK-10	nt	9.89	7.54	18.6	7.03	4.21	0.1
UO-31	0.58	2.56	4.31	4.37	3.59	2.41	0.019
Prostate							
PC-3	0.18	6.74	4.45	5.12	4.32	2.8	0.001
DU-145	0.1	8.97	2.04	4.11	2.51	3.81	0.001
Breast							
MCF7	0.051	2.3	2.88	2.89	3.16	0.74	0.005
MDA-MB-231	0.19	9.34	5.4	5.16	3.38	5.45	0.001
HS 578T	nt	na	4.15	4.33	4.18	4.32	0.001
BT-549	0.41	16.7	21.2	10.5	5.23	3.05	10
T-47D	1.0	3.39	4.03	3.95	4.79	9.41	10
MDA-MB-468	0.1	3.68	2.29	2.3	2.16	2.39	na

[a] Values are reported as GI_{50}, the micro molar concentration of the compound required to cause 50% inhibition of cell growth after an incubation time of 48 h.
[b] NSC 613729 (http://dtp.nci.nih.gov/dtpstandard/dwindex/index.jsp).
[c] NSC 753574.
[d] NSC 753576.
[e] NSC 753578.
[f] NSC 753581.
[g] NSC 753584.
[h] NSC 753587.
[i] nt = not tested.
[j] na = not active.

understand the effect of these conjugates on cell cycle, we have performed FACS analysis. In this study, MCF-7 cells were treated with compounds **11a**, **11b**, **11e**, **11f**, **11g**, **11h**, **11i**, **11j**, **11k**, **12b**, CA-4 and BT for 24 h at 4 μM concentration. CA-4 and BT compounds serves as starting materials. Compounds **11a**, **11b**, **11g**, **11h**, **11i** and **12b** have shown 46%, 42%, 37%, 43%, 38% and 37% of cell accumulation in G2/M phase (G2/M arrest). Whereas **11e**, **11f**, **11j** and **11k** exhibit 63%, 59%, 68% and 80% of cell accumulations in G1 phase respectively (G1 arrest). In control (untreated cells) 58% and 35% of accumulation in G1 and G2/M phases were observed, respectively (Fig. 3). This data clearly indicated that majority of the compounds showed G2/M cell cycle arrest with the exception of **11e**, **11f**, **11j** and **11k**. It is obvious that the variation in cell cycle arrest depends on the nature of compound as well as response of the cell type towards the specific compound of interest.

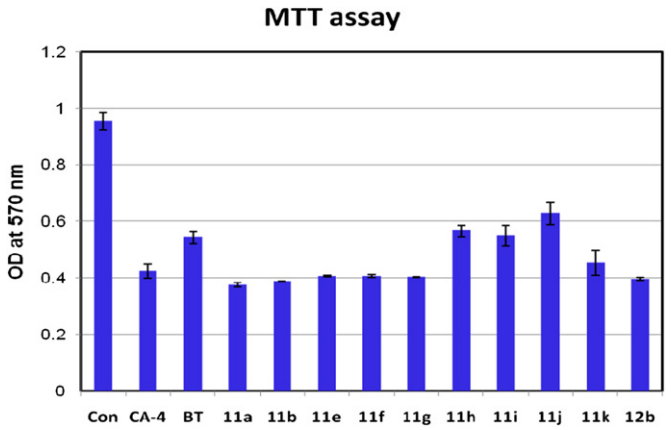

Fig. 2. Effect of combretastatin-benzothiazole conjugates on cell viability. MCF-7 cells were treated with compounds (**11a**, **11b**, **11e**, **11f**, **11g**, **11h**, **11i**, **11j**, **11k** and **12b**) at 4 μM concentration for 24 h in 96 well plates at 10,000 cells per well followed by MTT assay. Here the O.D directly indicates the cell viability after compound treatment. CA-4 was used as standard control. Control indicates the untreated cells. BT indicates 2-aminobenzothiazole.

2.2.3. Effect of compound 11a on tubulin polymerization

In General G2/M cell cycle arrest is strongly associated with inhibition of tubulin polymerization [39] and compound **11a** is most effective in causing G2/M cell cycle arrest, it was considered of interest to understand the microtubule inhibitory function of **11a**. To evaluate inhibitory activity of compound **11a** on tubulin polymerization, we have employed the HTS tubulin polymerization assay, where inhibition was shown as decrease in optical density (O.D). Here tubulin is dissolved in G-PEM buffer and incubated with compounds (**11a**, CA-4, Noc, and Pac), and readings were taken by photometry based method at a wavelength of 340 nm. It was observed that compound **11a** showed good tubulin inhibition (IC_{50}, 5 μM) that is comparable to CA-4. Here paclitaxel (Pac) was used as tubulin polymerization stabilizer (Fig. 4). Additionally, immunofluoresence analysis against tubulin was also examined for compound **11a** in MCF-7 cells. Therefore, the cells were treated with CA-4, nocodozole (Noc), paclitaxel (Pac), 2-aminobenzothiazole (BT) and **11a** at 4 μM concentration for 24 h. Compound **11a** has shown dispersed microtubule organization when compared to control (untreated cells). Nocodazole, a tubulin polymerization inhibitor and paclitaxel, a tubulin stabilizer were employed as negative and positive controls respectively (Fig. 5).

2.2.4. Effect of conjugates on c-Jun and ERK

ERK protein was found to be associate with kinetochore of mitotic spindles [40–44] and is needed for Mitotic Progression [45,46]. Previous studies [47,48] have shown that microtubule inhibitors cause specific as well as distinct effects on ERK pathway and combined effect leads to cause effective cell death [49]. c-Jun is a component of the activator protein (AP-1) and is associated with angiogenesis that is dispensable for the invasiveness in breast cancer [50]. Whereas ERK1/2 are the members of MAPK family proteins that control the cell division and are considered to provide survival signals which ultimately end in increased proliferation rate of the tumour [51]. Thus these proteins (ERK and c-Jun) contribute to metastasis in breast cancer [7]. Thus it was considered of interest to understand the molecular mechanism behind the cytotoxic nature of these conjugates. In this pursuit, MCF-7 cells were treated

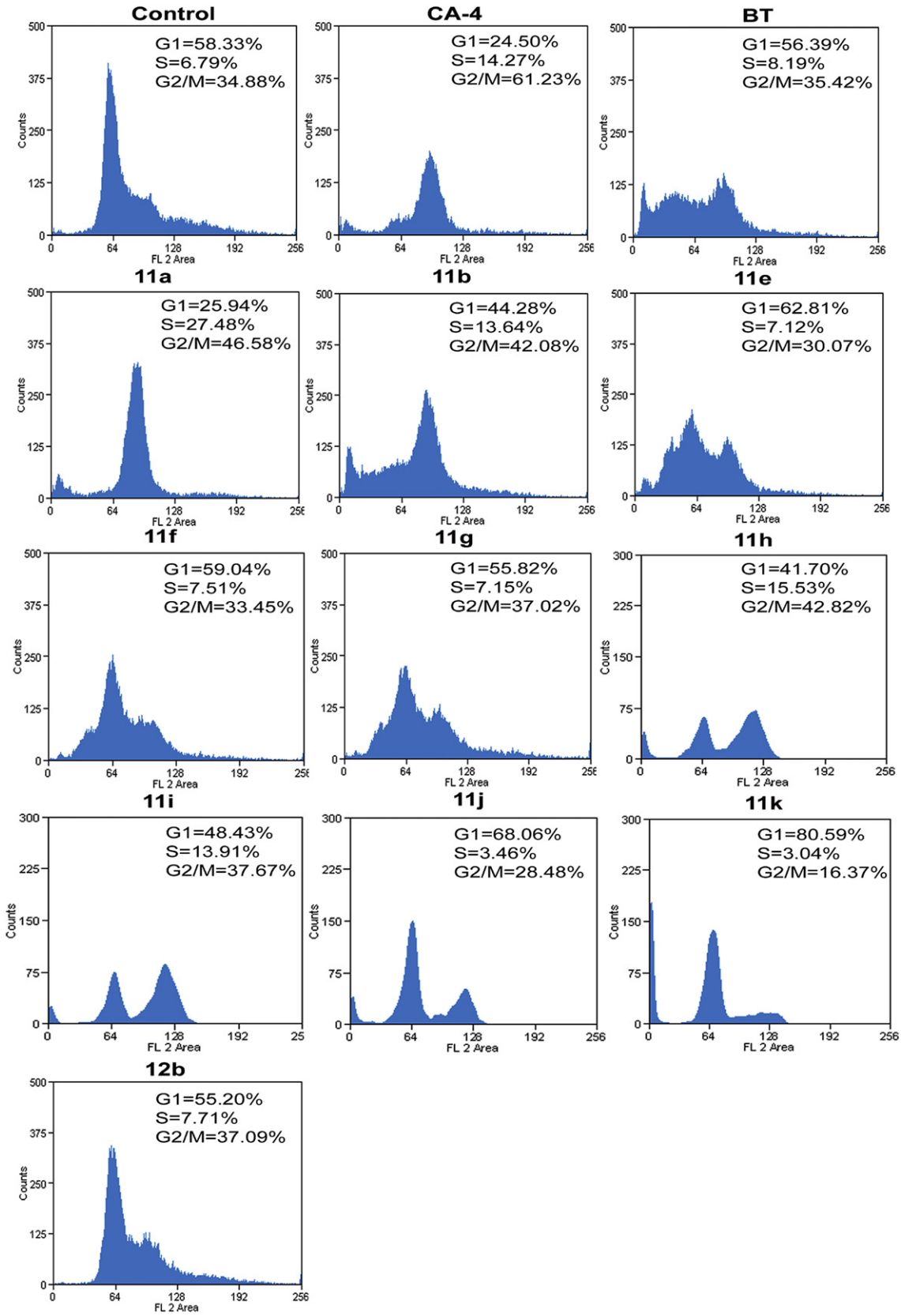

Fig. 3. FACS analysis of cell cycle distribution of MCF-7 cells after treatment with combretastatin-benzothiazole conjugates at 4 μM concentration for 24 h. CA-4 and BT (2-aminobenzothiazole) are the precursor molecules employed. Compounds **11a**, **11b**, **11g**, **11h**, **11i** and **12b** show G2/M arrest whereas compounds **11e**, **11f**, **11j** and **11k** show G1 arrest.

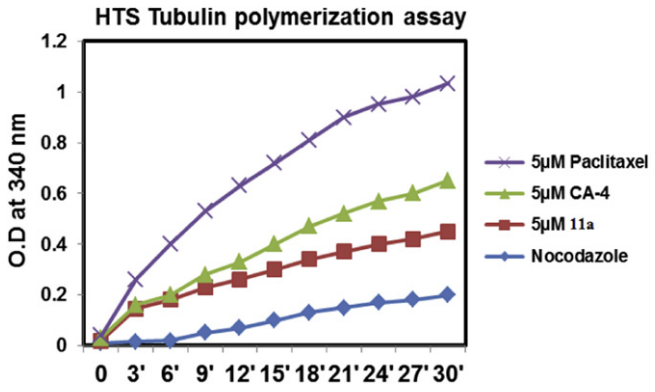

Fig. 4. Inhibitory activity of 11a on tubulin polymerization. In vitro HTS tubulin polymerization assay was carried out using 4 μM concentration of compounds CA-4, nocadazole, paclitaxel and 11a. Compounds were incubated with 100 μl of tubulin (dissolved in GPEM buffer) provided in the kit. The O.D was taken at 340 nm and is measure for the tubulin inhibitory activity.

with compounds CA-4, BT, **11a** and **11b** at 4 μM for 24 h followed by Western blot analysis. It was observed that there was a decrease in the level of ERK and c-Jun proteins in compound treated cells (Fig. 6).

Further, the effect of these compounds on phosphorylated (activated) form of ERK1/2 was examined, which up on entry in to the nucleus phosphorylate many proteins that cause rapid proliferation [2–4]. In this study as well, we found a decrease in phosphorylated form of ERK1/2 (Fig. 6). Additionally, immunofluorescence analysis against phosphorylated ERK1/2 in **11a** treated MCF-7 cells was also examined. It was surprising to observe that the retention of phosphorylated ERK1/2 form in the cytoplasm as shown in Fig. 7 revealed the inhibitory role of **11a** on ERK pathway.

2.2.5. Molecular modeling

To determine the possible binding modes of this series of compounds with ERK kinase, docking studies were carried out with the most potent compounds. These conjugates were docked in ATP binding pocket of ERK2. Biological activity studies suggested that compounds **11a** and **11b** were potent, hence we examined their interaction in ATP binding pocket of ERK2 (Fig. 8). Docking followed by molecular dynamics of the ATP binding pocket of ERK2 suggested that benzothiazole moiety was buried in the gorge of the ATP binding pocket forming several hydrophobic interactions with surrounding residues such as Val39, Ala52, Leu107, Met108, Leu156 and a polar interaction with Gln105. The combretastatin moiety also gets well tugged in the ATP binding pocket and provided a series of polar interactions with several residues that included Arg67, Lys54 and Cys166, while residues Tyr113 and Lys114 were involved in hydrophobic interactions. Interestingly, the interactions with gate keeper residues Val39, Lys54 and Gln105 were considered to be critical for the inhibitor selectivity. During molecular dynamics, 1.5–2.0 Å movement was observed in the loop near Cys166 towards the inhibitor, while region around Tyr36 moved away by 2.5–3.0 Å. Tight binding of benzothiazole moiety deep inside the ATP binding pocket suggested that any small change in the substituent could prove sensitive towards the inhibition of the enzyme. This modeling data provides a basis for possible interaction between the ERK and inhibitors.

The modeling studies on tubulin protein were carried out to evaluate binding modes in order to support the inhibition of tubulin polymerization. Compounds (**11a** and **11b**) were directly docked in the colchicine binding site of tubulin and the proposed binding sites located at the interface with the α-β subunit (Fig. 9). The trimethoxy phenyl ring of these compounds is surrounded by Cys241, Lys254, Leu255, Asn258, Leu248, Val318, Ala354 and Ile378. The Cys241 forms a hydrogen bond (S–H–O) with one of the methoxy oxygen atoms of trimethoxyphenyl ring of **11a** or **11b**. The benzothiazole amide moiety of both compounds move towards interface of α–β chain of tubulin. The keto group of amide forms a series of hydrogen bonds with Ser178 and Tyr224 of α-chain of tubulin while nitrogen atom of amide also participates in hydrogen bond with main chain of Gln247 of β-chain. Based on the modeling, it is clear that these molecules fit well in the tubulin α–β interface thereby allowing favorable interactions.

3. Conclusion

In the present study, a new series of combretastatin-amidobenzothiazole conjugates were synthesized. The compounds (**11a**, **11b**, **11e**, **11f**, **11g** and **12b**) showed potent anticancer activity against different human cancer cell lines. The cell viability assay of the two promising compounds **11a** and **11b** have shown potent cytotoxicity in MCF-7 cells at 4 μM. The FACS analysis of these compounds caused accumulation of cells in G2/M phase. It was observed from the results of biological assays that the active compounds have showed significant effect on tubulin polymerization as well as ERK signaling pathway. The c-Jun and ERK1/2 protein levels decreased upon treatment with compounds **11a** and **11b** in MCF-7 cells and more pronounced in case of **11a**. Interestingly, these compounds caused the decrease in phosphorylated forms of ERK1/2 protein and also prevented phospho-ERK to enter the nucleus which resulted in retention of this phospho-ERK in cytoplasm, thereby controlling the abnormal cell proliferation [52]. Moreover these conjugates also exhibited inhibitory activity on c-Jun protein. From the studies of biological assays, it may conclude that the significant anticancer activity exhibited by this compound is combined effect of both tubulin polymerization inhibition and ERK inhibition. From molecular modeling studies it was demonstrated that these molecules bound well in the ATP binding pocket and were involved in a series of interactions with the protein providing the molecular basis for inhibition of ERK. The modeling study on tubulin demonstrated that these molecules bind well with the tubulin and are involved in a series of interactions with the protein. Thus these conjugates could be considered as potential leads in the development of a new class of anticancer therapeutics [53].

4. Experimental section

All chemicals and reagents were obtained from Aldrich (Sigma–Aldrich, St. Louis, MO, USA), Lancaster (Alfa Aesar, Johnson Matthey Company, Ward Hill, MA, USA) or Spectrochem Pvt. Ltd (Mumbai, India) and were used without further purification. Reactions were monitored by TLC, performed on silica gel glass plates containing 60GF-254, and visualization on TLC was achieved by UV light or iodine indicator. Column chromatography was performed with Merck 60–120 mesh silica gel. ^{1}H NMR and ^{13}C NMR spectra were recorded on Gemini Varian-VXR-unity (200 MHz) or Bruker UXNMR/XWIN-NMR (300 MHz) instruments. Chemical shifts (δ) are reported in ppm downfield from internal TMS standard. ESI spectra were recorded on Micro mass, Quattro LC using ESI + software with capillary voltage 3.98 kV and ESI mode positive ion trap detector. High-resolution mass spectra (HRMS) were recorded on QSTAR XL Hybrid MS/MS mass spectrometer. Melting points were determined with an Electro thermal melting point apparatus, and are uncorrected.

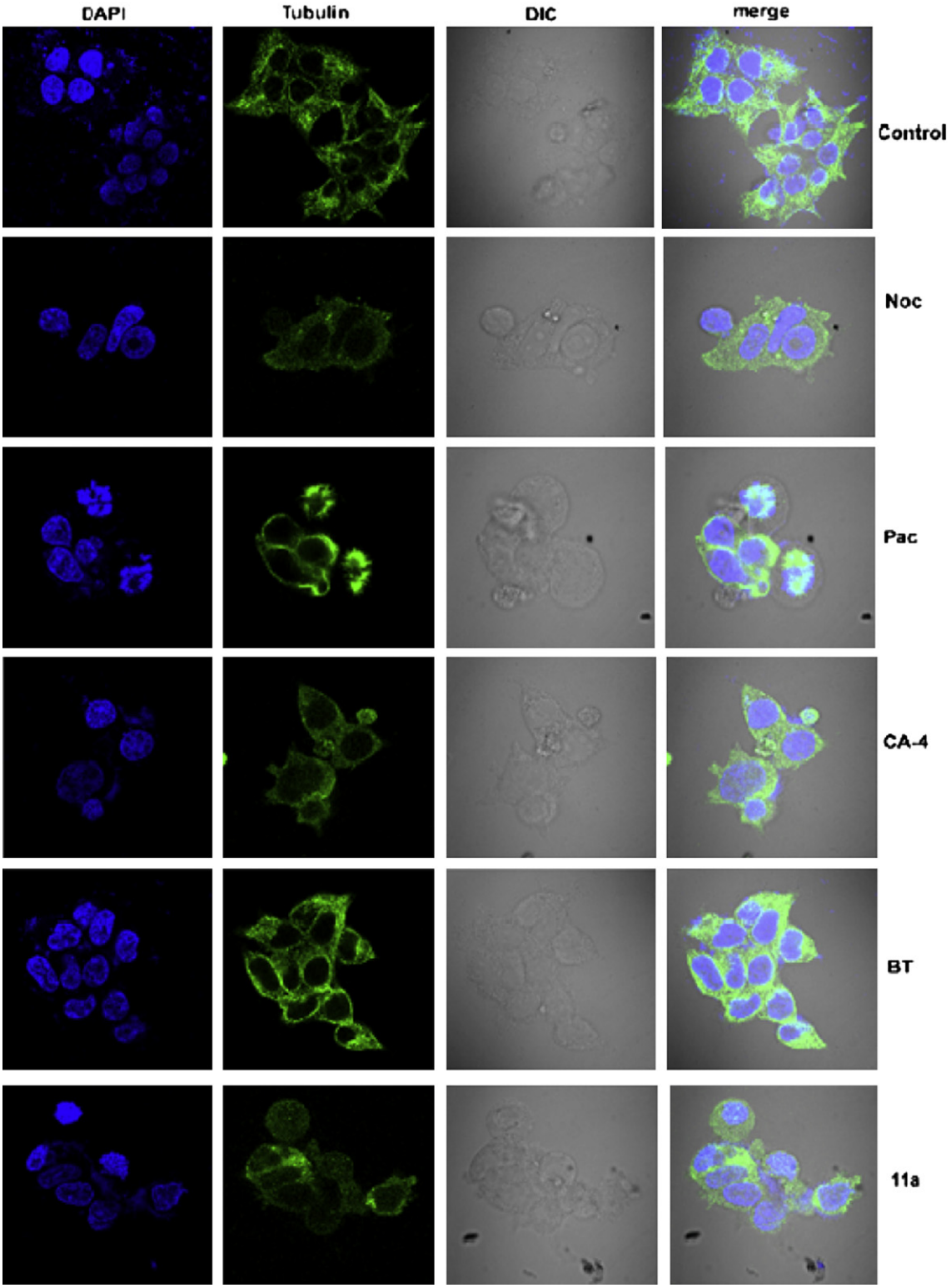

Fig. 5. Effect of compound on the microtubule network: MCF-7 cells were treated with compound **11a**, combretastatin (CA-4), 2-aminobenzothiazole (BT), nocodazole (Noc), and paclitaxel (Pac) at 4 μM concentration for 24 h. This is followed by staining with α-tubulin antibody. Microtubule organization was clearly observed by green colored tubulin network like structures in control cells and was found to be disrupted in nocodazole and **11a** treated cells. Paclitaxel works as microtubule stabilization (i.e. bundling of tubulin). BT did not show any effect on tubulin polymerization and acted like control untreated cells. (For interpretation of the references to color in this figure legend, the reader is referred to the web version of this article.)

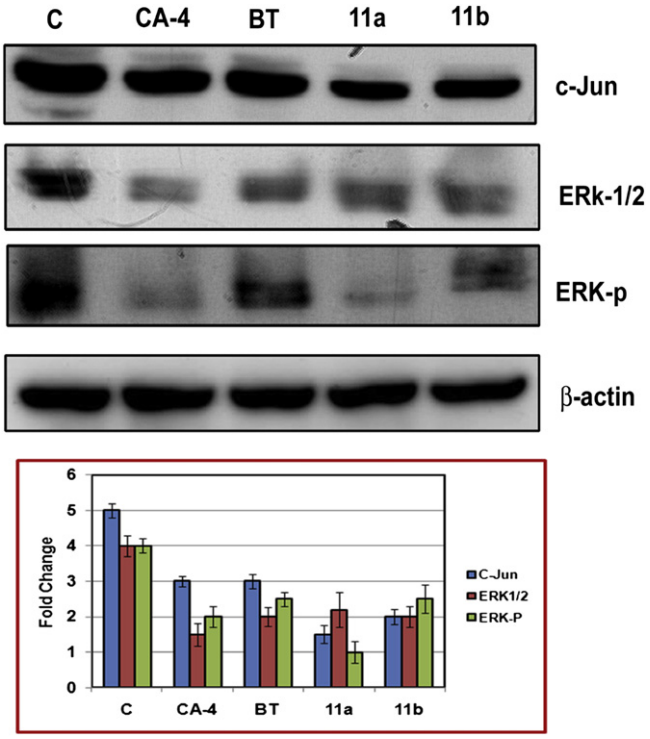

Fig. 6. Compounds **11a** and **11b** inhibit c-Jun, ERK and ERK-p (phosphorylated ERK) protein expression. Here MCF-7 cells were treated with compounds CA-4, BT (2-aminobenzothiazole), **11a** and **11b** at 4 μM concentration for 24 h before subjected to Western blot analysis.

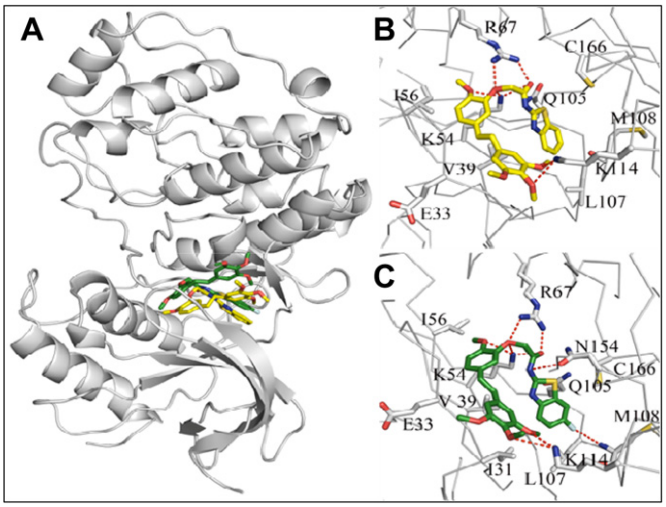

Fig. 8. Molecular modeling of **11a** (yellow) and **11b** (green) in complex with ERK2. A). Overall structure is shown in grey cartoon diagram while, compounds and the surrounding residues are displayed in sticks. B). Represented MD trajectory snapshot of ERK2-**11a** complex. C) Represented MD trajectory snapshot of ERK2-**11b** complex. For the sake of clarity all amino acids.

*4.1. (Z)-tert-butyl(2-methoxy-5-(3,4,5-rimethoxystyryl)phenoxy) dimethylsilane (**8a**)*

To a solution of compound **7** (593 mg, 1.0 mmol) and trimethoxybenzaldehyde (196 mg, 1.0 mmol) in dry dichloromethane (15 mL) was cooled to 0 °C and added NaH (29 mg, 1.2 mmol). The reaction mixture was stirred for 14 h at room temperature. The reaction was monitored by TLC using ethyl acetate and hexane. After completion of the reaction, the reaction mixture was

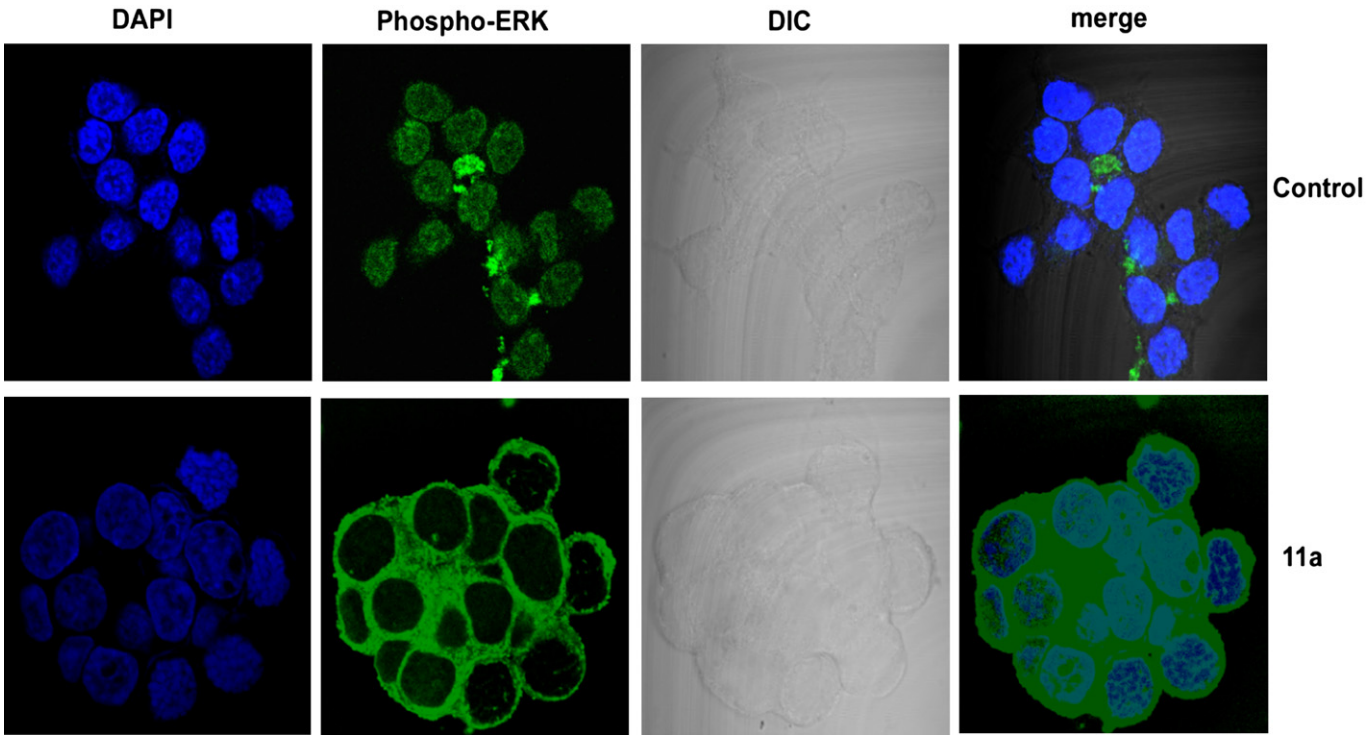

Fig. 7. Compound **11a** inhibits the nuclear translocation of phosphorylated form of ERK. MCF-7 cells were treated with 4 μM concentration of compound **11a** for 24 h and subjected to immunofluorescence procedure using phospho-ERK antibody.

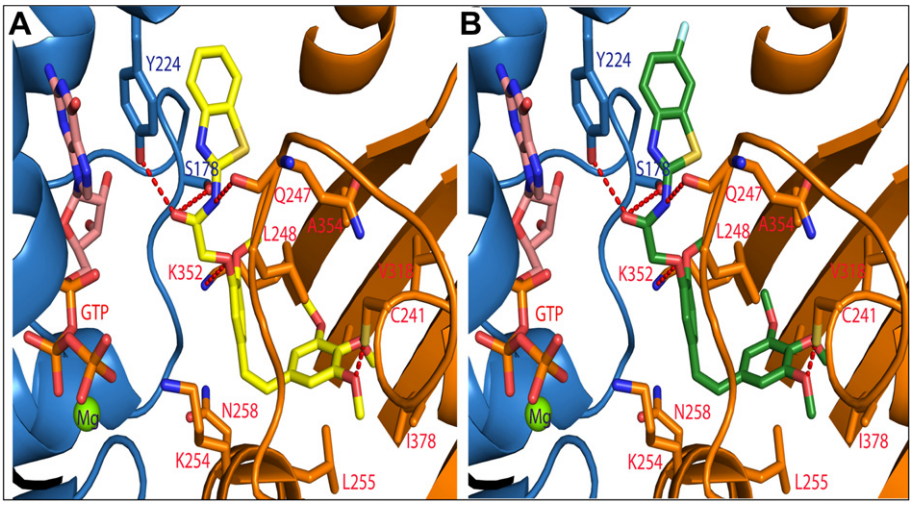

Fig. 9. (A) Docking position of **11a** (yellow) in the colchicine-binding site of tubulin; (B) Docking position of **11b** (green) in the colchicine-binding site of tubulin. Blue cartoon represent α-chain of tubulin while orange represent β-chain of tubulin. Red dotted lines represent possible hydrogen bonds between protein and ligands. (For interpretation of the references to color in this figure legend, the reader is referred to the web version of this article.)

quenched with ice water and extracted with ethyl acetate (2 × 20 ml). The combined organic phases were washed with water followed by brine solution, dried over Na_2SO_4 and evaporated under vacuum to afford crude product. The crude product was a mixture of *Z*- and *E*- isomers. The *Z*- isomer was separated by flash column chromatography using hexane:ethyl acetate (19:1) as a solvent system to obtain the pure product **8a** (120 mg, 40% yield) as viscous liquid followed by compound **8b** (241 mg, 60% yield) as white solid. Compound **8a:** ^{1}H NMR (200 MHz, $CDCl_3$): δ = 6.76–6.82 (dd, 1H, J = 8.3, 2.2 Hz), 6.73 (d, 1H, J = 2.2 Hz), 6.69 (d, 1H, J = 8.3 Hz), 6.39–6.46 (m, 3H), 6.36 (d, 1H, J = 12.0 Hz), 3.79 (s, 3H), 3.77 (s, 3H), 3.69 (s, 6H), 0.96 (s, 9H), 0.14 (s, 6H); MS (ESI): m/z 431 $[M+1]^+$; Compound **8b:** ^{1}H NMR (200 MHz, $CDCl_3$): δ = 6.71 (s, 2H), 6.91 (d, 1H, J = 15.8 Hz), 6.85 (d, 1H, J = 15.8 Hz), 6.83 (d, 1H, J = 8.3 Hz), 7.02–7.09 (m, 2H), 3.91 (s, 6H), 3.87 (s, 3H), 3.82 (s, 3H), 1.03 (s, 9H), 0.19 (s, 6H); MS (ESI): m/z 431 $[M+1]^+$.

4.2. Trans to cis isomerization of compound (*8b*) [34]

The *trans* compound **8b** (2 g) was dissolved in ethanol (1 L). The solution was kept under sunlight for 6–7 h. After completion of the reaction as indicated by TLC, ethanol was distilled under reduced pressure and purified by flash column chromatography using hexane:ethyl acetate (19:1) as a solvent system to obtain the pure *cis* isomer **8a** as viscous liquid (1.44 g, 72% yield).

4.3. (Z)-2-methoxy-5-(3,4,5-trimethoxystyryl)phenol (*2*)

To a solution of compound **8a** (430 mg, 1.0 mmol) in dry THF (15 mL) was added TBAF solution (1.5 ml, 1 M solution in THF) under cooling conditions and stirred for 20 min at 5–10 °C. The reaction was monitored by TLC using ethyl acetate:hexane. After completion of the reaction as indicated by the TLC, the reaction mixture was quenched with sodium bicarbonate solution and extracted with ethyl acetate (2 × 20 ml). The combined organic phases were washed with water followed by brine solution, dried over Na_2SO_4 and evaporated under vacuum to afford crude product of **2**. This was further purified by column chromatography using hexane:ethyl acetate (2:8) as a solvent system to obtain the pure product **2** (251 mg, 79% yield); ^{1}H NMR (200 MHz, $CDCl_3$): δ = 6.92 (d, 1H, J = 2.2 Hz), 6.77–6.83 (dd, 1H, J = 8.3, 1.5 Hz), 6.73 (d, 1H, J = 8.3 Hz), 6.53 (s, 2H), 6.47 (d, 1H, J = 12.0 Hz), 6.41 (d, 1H, J = 12.0 Hz), 5.57 (br s, 1H), 3.86 (s, 3H), 3.84 (s, 3H), 3.7 (s, 6H); MS (ESI): m/z 317 $[M+1]^+$.

4.4. (Z)-ethyl-2-(2-methoxy-5-(3,4,5-trimethoxystyryl)phenoxy) acetate (*9*)

To a solution of compound **2** (316 mg, 1.0 mmol) in dry DMF (10 mL) was added anhydrous K_2CO_3 (276 mg, 2.0 mmol) and α-bromoethyl acetate (250 mg, 1.5 mmol) and the mixture was stirred at room temperature for 24 h. The reaction was monitored by TLC using ethyl acetate:hexane (6:4). After completion of the reaction as indicated by the TLC, K_2CO_3 was removed by filtration, diluted with water and extracted with dichloromethane (2 × 20 ml). The combined organic phases were washed with water followed by brine solution, dried over Na_2SO_4 and evaporated under vacuum. The residue, thus obtained was purified by column chromatography using ethyl acetate and hexane (7:3) to afford pure compound **9** (380 mg, 94% yield); ^{1}H NMR (300 MHz, $CDCl_3$): δ = 6.83–6.89 (dd, 1H, J = 8.3, 1.5 Hz), 6.75 (d, 1H, J = 8.3 Hz), 6.7 (d, 1H, J = 1.5 Hz), 6.4–6.46 (m, 3H), 6.47 (d, 1H, J = 12.0 Hz), 4.44 (s, 2H), 4.11–4.20 (q, 2H), 3.85 (s, 3H), 3.8 (s, 3H), 3.69 (s, 6H), 1.24 (t, 3H, J = 7.5, 6.7 Hz); MS (ESI): m/z 403 $[M+1]^+$.

4.5. (Z)-2-(2-methoxy-5-(3,4,5-trimethoxystyryl)phenoxy)acetic acid (*10*)

To a solution of compound **9** (402 mg, 1.0 mmol) in THF (10 ml) and water (2 ml), LiOH.H_2O (84 mg, 2.0 mmol) was added, and the mixture was stirred at room temperature for 12 h. The reaction was monitored by TLC using ethyl acetate. After completion of the reaction as indicated by the TLC, the solvent was removed under vacuum and neutralized with dilute HCl up to pH 7. After neutralization the reaction mixture was extracted with dichloromethane (2 × 20 ml). The combined organic phases were washed with water followed by brine solution, dried over Na_2SO_4 and evaporated under vacuum to obtain crude compound **10**. This compound was purified by recrystallization by using ethyl acetate as solvent to obtain the pure product **10** (302 mg, 80% yield); ^{1}H NMR (200 MHz, $CDCl_3$): δ = 7.96 (br s, 1H), 6.84–6.9 (dd, 1H, J = 8.3, 1.5 Hz), 6.77 (d,

1H, $J = 8.3$ Hz), 6.72 (d, 1H, $J = 1.5$ Hz), 6.31–6.49 (m, 4H), 4.47 (s, 2H), 3.86 (s, 3H), 3.8 (s, 3H), 3.69 (s, 6H); MS (ESI): m/z 375 $[M+1]^+$.

4.6. (Z)-N-(benzo[d]thiazol-2-yl)-2-(2-methoxy-5-(3,4,5-trimethoxy styryl)phenoxy)acetamide (**11a**)

To a solution of compound 2-aminobenzothiazole (150 mg, 1.0 mmol) in dichloromethane (20 ml) was added 1-(3-Dimethyl aminopropyl)-3-ethylcarbodiimide (EDCI) (210 mg, 1.1 mmol) and 1-hydroxy-1,2,3-benzotriazole (HOBt) (13.5 mg, 0.1 mmol). Then added (Z)-2-(2-methoxy-5-(3,4,5-trimethoxystyryl) phenoxy)acetic acid **10** (374 mg, 1.0 mmol) and the reaction mixture was stirred at room temperature for 24 h and the reaction was monitored by TLC. After completion of reaction, water was added to reaction mixture and extracted with dichloromethane (2 × 30 ml). The solvent was evaporated under vacuum to afford the crude product. This was further purified by column chromatography using ethyl acetate and hexane (1:1) as solvent system to obtain the pure product **11a** (449 mg, 88% yield) as white solid; mp: 113–115 °C; ^{1}H NMR (200 MHz, $CDCl_3$): $\delta = 7.74$–7.82 (m, 2H), 7.37–7.44 (m, 1H), 7.29 (d, 1H, $J = 8.3$ Hz), 6.96–7.01 (d, 1H, $J = 8.3$, 2.2 Hz), 6.93 (d, 1H, $J = 2.2$ Hz), 6.82 (d, 1H, $J = 8.3$ Hz), 6.46 (d, 1H, $J = 12.0$ Hz), 6.38–4.3 (m, 3H), 4.60 (s, 2H), 4.02 (s, 3H), 3.83 (s, 3H), 3.69 (s, 6H); ^{13}C NMR (75 MHz, $CDCl_3$): δ= 167.54, 156.73, 152.98, 149.06, 148.47, 146.60, 137.29, 132.45, 132.20, 130.43, 129.70, 128.61, 126.19, 124.99, 124.05,121.36, 121.18, 118.14, 111.62, 105.81, 70.40, 60.92, 55.90; IR (KBr) (ν_{max}/cm^{-1}): 3390, 2924, 1696, 1582, 1548, 1508, 1422, 1325, 1261, 1130, 1017, 882, 801, 755; MS (ESI): m/z 507 $[M+1]^+$; HRMS (ESI m/z) $[M+1]^+$ calcd for $C_{27}H_{27}N_2O_6S$: 507.1589, found: 507.1585.

4.7. (Z)-2-(2-methoxy-5-(3,4,5-trimethoxystyryl)phenoxy)-N-(6-fluorobenzo[d]thiazol-2-yl) acetamide (**11b**)

This compound was prepared according to the method described for compound **11a** by employing (Z)-2-(2-methoxy-5-(3,4,5-trimethoxystyryl) phenoxy)acetic acid (**10**) (374 mg, 1.0 mmol), and 2-amino-6-fluoro benzothiazole (168 mg, 1.0 mmol) to obtain the pure product **11b** (428 mg, 93% yield) as white solid; mp: 115–117 °C; ^{1}H NMR (300 MHz, $CDCl_3$): $\delta = 7.71$–7.76 (m, 1H), 7.47–7.53 (dd, 1H, $J = 8.1$, 2.4 Hz), 7.13–7.2 (m, 1H), 7–7.04 (dd, 1H, $J = 8.1$, 1.6 Hz), 6.93 (d, 1H, $J = 1.6$ Hz), 6.83 (d, 1H, $J = 8.1$ Hz), 6.46–6.51 (m, 3H), 6.44 (d, 1H, $J = 12.2$ Hz), 4.63 (s, 2H), 3.98 (s, 3H), 3.85 (s, 3H), 3.70 (s, 6H); ^{13}C NMR (75 MHz, $CDCl_3$): δ = 167.63, 161.26, 158.04, 156.41, 152.99, 149.04, 146.60, 144.91, 137.24, 132.47, 130.49, 129.75, 128.58, 125.07, 121.99, 118.25, 114.77, 111.66, 107.47, 105.81, 70.46, 60.9, 55.89; IR (KBr) (ν_{max}/cm^{-1}): 3360, 2929, 1712, 1608, 1578, 1553, 1513, 1458, 1261, 1126, 1024, 996, 883, 812, 674; MS (ESI): m/z 525 $[M+1]^+$; HRMS (ESI m/z) $[M+1]^+$ calcd for $C_{27}H_{26}N_2O_6FS$: 525.1495, found: 525.1483.

4.8. (Z)-2-(2-methoxy-5-(3,4,5-trimethoxystyryl)phenoxy)-N-(6-chlorobenzo[d]thiazol-2-yl) acetamide (**11c**)

This compound was prepared according to the method described for compound **11a** by employing (Z)-2-(2-methoxy-5-(3,4,5-trimethoxystyryl) phenoxy)acetic acid (**10**) (374 mg, 1.0 mmol), and 2-amino-6-chloro benzothiazole (184 mg, 1.0 mmol) to obtain the pure product **11c** (502 mg, 92% yield) as white solid; mp: 114–117 °C; ^{1}H NMR (200 MHz, $CDCl_3$): $\delta = 7.8$ (d, 1H, $J = 2.2$ Hz), 7.73 (d, 1H, $J = 9$ Hz), 7.38–7.44 (dd, 1H, $J = 8.3$, 2.2 Hz), 7.0–7.06 (dd, 1H, $J = 8.3$, 2.2 Hz), 6.94 (d, 1H, $J = 2.2$ Hz), 6.84 (d, 1H, $J = 9.0$ Hz), 6.42–6.54 (m, 4H), 4.64 (s, 2H), 3.98 (s, 3H), 3.85 (s, 3H), 3.7 (s, 6H); ^{13}C NMR (75 MHz, $CDCl_3$): δ = 167.94, 160.37, 153.0, 149.02, 146.53, 145.93, 137.31, 132.85, 132.43, 130.53, 129.94, 129.72, 128.65, 127.22, 125.03, 121.72, 121.08, 118.10, 111.76, 105.96, 70.21, 60.91, 56.0; IR (KBr) (ν_{max}/cm^{-1}): 3360, 2931, 1714, 1597, 1543, 1511, 1442, 1426, 1325, 1262, 1235, 1124, 1023, 996, 879, 818, 765, 668; MS (ESI): m/z 541 $[M]^+$; HRMS (ESI m/z) $[M+1]^+$ calcd for $C_{27}H_{26}N_2O_6SCl$: 541.1200, found: 541.1224.

4.9. (Z)-2-(2-methoxy-5-(3,4,5-trimethoxystyryl)phenoxy)-N-(6-nitrobenzo[d]thiazol-2-yl) acetamide (**11d**)

This compound was prepared according to the method described for compound **11a** by employing (Z)-2-(2-methoxy-5-(3,4,5-trimethoxystyryl) phenoxy)acetic acid (**10**) (374 mg, 1.0 mmol), and 2-amino-6-nitro benzothiazole (195 mg, 1.0 mmol) to obtain the pure product **11d** (500 mg, 90% yield) as yellow solid; mp: 117–119 °C; ^{1}H NMR (300 MHz, $CDCl_3$): $\delta = 11.03$ (s, 1H), 8.77 (d, 1H, $J = 2.1$ Hz), 8.32–8.36 (dd, 1H, $J = 8.7$, 2.1 Hz), 7.88 (d, 1H, $J = 8.7$ Hz), 7.03–7.07 (dd, 1H, $J = 8.0$, 2.1 Hz), 6.97 (d, 1H, $J = 2.1$ Hz), 6.87 (d, 1H, $J = 8.0$ Hz), 6.52 (d, 1H, $J = 12.4$ Hz), 6.49 (s, 2H), 6.46 (d, 1H, $J = 12.4$ Hz), 4.68 (s, 2H), 4.02 (s, 3H), 3.86 (s, 3H), 3.71 (s, 6H); IR (KBr) (ν_{max}/cm^{-1}): 3353, 2927, 1708, 1575, 1533, 1510, 1446, 1427, 1337, 1265, 1124, 1043, 878, 751, 659; MS (ESI): m/z 552 $[M+1]^+$; HRMS (ESI m/z) $[M + Na]^+$ calcd for $C_{27}H_{25}N_3O_8SNa$: 574.1260, found: 574.1279.

4.10. (Z)-2-(2-methoxy-5-(3,4,5-trimethoxystyryl)phenoxy)-N-(6-methoxybenzo[d]thiazol-2-yl)acetamide (**11e**)

This compound was prepared according to the method described for compound **11a** by employing (Z)-2-(2-methoxy-5-(3,4,5-trimethoxystyryl) phenoxy)acetic acid (**10**) (374 mg, 1.0 mmol), and 2-amino-6-methoxy benzothiazole (180 mg, 1.0 mmol) to obtain the pure product **11e** (480 mg, 89% yield) as white solid; mp: 114–117 °C; ^{1}H NMR (300 MHz, $CDCl_3$): $\delta = 7.71$ (d, 1H, $J = 9.0$ Hz), 7.30 (d, 1H, $J = 2.2$ Hz), 6.99–7.1 (m, 2H), 6.94 (d, 1H, $J = 2.2$ Hz), 6.84 (d, 1H, $J = 8.3$ Hz), 6.43–6.53 (m, 4H), 4.63 (s, 2H), 3.98 (s, 3H), 3.88 (s, 3H), 3.85 (s, 3H), 3.7 (s, 6H); ^{13}C NMR (75 MHz, $CDCl_3$): δ = 186.55, 176.15, 174.09, 172.20, 168.29, 165.82, 161.62, 156.45, 152.54, 151.72, 149.63, 148.92, 147.88, 144.14, 140.90, 137.24, 134.54, 130.86, 125.04, 123.38, 89.50, 80.16, 75.15, 75.02, 48.87; IR (KBr) (ν_{max}/cm^{-1}): 3381, 2927, 1688, 1606, 1579, 1550, 1508, 1429, 1325, 1262, 1125, 1059, 879, 820, 784; MS (ESI): m/z 537 $[M + 1]^+$; HRMS (ESI m/z) $[M+1]^+$ calcd for $C_{28}H_{29}N_2O_7S$: 537.1695, found: 537.1677.

4.11. (Z)-2-(2-methoxy-5-(3,4,5-trimethoxystyryl)phenoxy)-N-(6-trifluoromethoxybenzo[d] thiazol-2-yl)acetamide (**11f**)

This compound was prepared according to the method described for compound **11a** by employing (Z)-2-(2-methoxy-5-(3,4,5-trimethoxystyryl)phenoxy)acetic acid (**10**) (374 mg, 1.0 mmol), and 2-amino-6-trifluoromethoxy benzothiazole (234 mg, 1.0 mmol) to obtain the pure product **11f** (550 mg, 93% yield) as white solid; mp: 122–124 °C; ^{1}H NMR (300 MHz, $CDCl_3$): $\delta = 7.8$ (d, 1H, $J = 8.8$ Hz), 7.69 (s, 1H), 7.29–7.36 (dd, 1H, $J = 8.4$, 2.2 Hz), 7.01–7.06 (dd, 1H, $J = 8.4$, 1.7 Hz), 6.95 (d, 1H, $J = 1.7$ Hz), 6.85 (d, 1H, $J = 8.3$ Hz), 6.42–6.53 (m, 4H), 4.65 (s, 2H), 3.99 (s, 3H), 3.85 (s, 3H), 3.7 (s, 6H); ^{13}C NMR (75 MHz, $CDCl_3$): δ = 167.82, 157.64, 153.03, 149.08, 147.14, 146.66, 145.5, 137.29, 133.09, 132.5, 130.57, 129.82, 128.59, 125.2, 121.96, 120.16, 118.42, 114.21, 111.70, 105.8, 103.38, 70.59, 60.96, 55.95; IR (KBr) (ν_{max}/cm^{-1}): 3389, 2924, 1697, 1613, 1580, 1551, 1508, 1457, 1261, 1130, 10174, 868, 811, 783, 669, 638; MS (ESI): m/z 591 $[M+1]^+$; HRMS (ESI m/z) $[M+1]^+$ calcd for $C_{28}H_{26}N_2O_7F_3S$: 591.1412, found: 591.1384.

*4.12. (Z)-2-(2-methoxy-5-(3,4,5-trimethoxystyryl)phenoxy)-N-(6-trifluoromethylbenzo[d] thiazol-2-yl)acetamide (**11g**)*

This compound was prepared according to the method described for compound **11a** by employing (Z)-2-(2-methoxy-5-(3,4,5-trimethoxystyryl)phenoxy)acetic acid (**10**) (374 mg, 1.0 mmol), and 2-amino-6-trifluoromethyl benzothiazole (218 mg, 1.0 mmol) to obtain the pure product **11g** (480 mg, 83% yield) as white solid; mp: 119–122 °C; ^{1}H NMR (200 MHz, $CDCl_3$): δ = 8.12 (s, 1H), 7.93 (d, 1H, J = 8.4 Hz), 7.69–7.75 (m, 1H), 7.01–7.06 (dd, 1H, J = 8.3, 1.7 Hz), 6.95 (d, 1H, J = 1.7 Hz), 6.85 (d, 1H, J = 8.3 Hz), 6.43–6.53 (m, 1H), 4.68 (s, 2H), 3.99 (s, 3H), 3.83 (s, 3H), 3.7 (s, 6H); ^{13}C NMR (75 MHz, $CDCl_3$): δ = 168.02, 1549.30, 153.02, 150.77, 149.07, 146.66, 137.32, 132.48, 132.31, 130.59, 129.80, 128.56, 126.01, 125.19, 123.29, 121.35, 119.10, 118.46, 111.72, 105.89, 103.43, 70.60, 60.91, 55.90; IR (KBr) (ν_{max}/cm^{-1}): 3377, 2925, 1706, 1580, 1535, 1508, 1465, 1320, 1267, 1164, 1126, 1084, 863, 824, 782, 668; MS (ESI): *m/z* 597 [M + Na]$^+$; HRMS (ESI *m/z*) [M+1]$^+$ calcd for $C_{28}H_{26}N_2O_6F_3$: 575.1463, found: 575.1446.

*4.13. (Z)-2-(2-methoxy-5-(3,4,5-trimethoxystyryl)phenoxy)-N-(6-methylbenzo[d] thiazol-2-yl)acetamide (**11h**)*

This compound was prepared according to the method described for compound **11a** by employing (Z)-2-(2-methoxy-5-(3,4,5-trimethoxystyryl)phenoxy)acetic acid (**10**) (374 mg, 1.0 mmol), and 2-amino-6-methyl benzothiazole (164 mg, 1.0 mmol) to obtain the pure product **11h** (451 mg, 81% yield) as white solid; mp: 112–114 °C; ^{1}H NMR (300 MHz, $CDCl_3$): δ = 7.64 (d, 1H, J = 9.1 Hz), 7.28 (d, 1H, J = 2.1 Hz), 6.91–7.02 (m, 2H), 6.89 (d, 1H, J = 2.2 Hz), 6.84 (d, 1H, J = 8.3 Hz), 6.42–6.55 (m, 4H), 4.63 (s, 2H), 3.87 (s, 3H), 3.84 (s, 3H), 3.71 (s, 6H), 2.49 (s, 3H); ^{13}C NMR (75 MHz, $CDCl_3$): δ = 185.9, 175.42, 174.01, 171.22, 168.21, 165.78, 161.44, 156.34, 152.54, 151.62, 149.54, 148.85, 147.75, 144.13, 140.92, 137.34, 134.65, 130.86, 125.12, 123.38, 80.16, 75.25, 75.02, 48.78, 28.3; MS (ESI): *m/z* 521 [M+1]$^+$; HRMS (ESI *m/z*) [M+1]$^+$ calcd for $C_{28}H_{28}N_2O_6S$: 521.1362, found: 521.1344.

*4.14. (Z)-2-(2-methoxy-5-(3,4,5-trimethoxystyryl)phenoxy)-N-(6-ethoxybenzo[d] thiazol-2-yl)acetamide (**11i**)*

This compound was prepared according to the method described for compound **11a** by employing (Z)-2-(2-methoxy-5-(3,4,5-trimethoxystyryl)phenoxy)acetic acid (**10**) (374 mg, 1.0 mmol), and 2-amino-6-ethoxy benzothiazole (194 mg, 1.0 mmol) to obtain the pure product **11i** (475 mg, 85% yield) as white solid; mp: 116–117 °C; ^{1}H NMR (300 MHz, $CDCl_3$): δ = 7.69 (d, 1H, J = 9 Hz), 7.29 (d, 1H, J = 2.4 Hz), 6.97–7.05 (m, 2H), 6.93 (d, 1H, J = 2.2 Hz), 6.83 (d, 1H, J = 8.3 Hz), 6.42–6.51 (m, 4H), 4.62 (s, 2H), 4.02–3.98 (q, 2H), 3.88 (s, 3H), 3.86 (s, 3H), 3.72 (s, 6H), 1.47 (t, 3H); ^{13}C NMR (75 MHz, $CDCl_3$): δ = 186.42, 176.34, 174.11, 172.22, 168.3, 165.82, 161.63, 156.51, 152.53, 151.72, 149.62, 148.9, 147.89, 144.23, 140.91, 137.21, 134.54, 130.81, 125.1, 123.37, 89.51, 80.19, 75.45, 75.09, 48.53, 31.2; MS (ESI): *m/z* 551 [M+1]$^+$; HRMS (ESI *m/z*) [M+1]$^+$ calcd for $C_{29}H_{30}N_2O_7S$: 551.1473, found: 551.1455.

*4.15. (Z)-2-(2-methoxy-5-(3,4,5-trimethoxystyryl)phenoxy)-N-(4-methylbenzo[d] thiazol-2-yl)acetamide (**11j**)*

This compound was prepared according to the method described for compound **11a** by employing (Z)-2-(2-methoxy-5-(3,4,5-trimethoxystyryl)phenoxy)acetic acid (**10**) (374 mg, 1.0 mmol), and 2-amino-4-methyl benzothiazole (164 mg, 1.0 mmol) to obtain the pure product **11j** (450 mg, 80% yield) as white solid; mp: 113–114 °C; ^{1}H NMR (300 MHz, $CDCl_3$): δ = 7.62–7.69 (m, 1H), 7.31–7.44 (m, 2H), 7.08 (d, 1H, J = 8.3 Hz), 6.91 (d, 1H, J = 2.3 Hz), 6.82 (d, 1H, J = 8.3 Hz), 6.41–6.52 (m, 4H), 4.61 (s, 2H), 3.88 (s, 3H), 3.85 (s, 3H), 3.7 (s, 6H), 2.62 (s, 3H); ^{13}C NMR (75 MHz, $CDCl_3$): δ = 186.1, 175.33, 174.23, 171.54, 167.65, 165.44, 161.12, 156.52, 152.97, 151.05, 149.27, 148.45, 147.64, 144.12, 140.87, 137.23, 134.57, 131.05, 125.43, 123.87, 80.97, 75.78, 74.25, 48.56, 27.38; MS (ESI): *m/z* 521 [M+1]$^+$; HRMS (ESI *m/z*) [M+1]$^+$ calcd for $C_{28}H_{28}N_2O_6S$: 521.1473, found: 521.1454.

*4.16. (Z)-2-(2-methoxy-5-(3,4,5-trimethoxystyryl)phenoxy)-N-(5,6-dimethylbenzo[d] thiazol-2-yl)acetamide (**11k**)*

This compound was prepared according to the method described for compound **11a** by employing (Z)-2-(2-methoxy-5-(3,4,5-trimethoxystyryl)phenoxy)acetic acid (**10**) (374 mg, 1.0 mmol), and 2-amino-5,6-dimethyl benzothiazole (178 mg, 1.0 mmol) to obtain the pure product **11k** (472 mg, 83% yield) as white solid; mp: 119–120 °C; ^{1}H NMR (300 MHz, $CDCl_3$): δ = 8.14 (s, 1H), 8.02 (s, 1H), 6.75 (d, 1H, J = 2.2 Hz), 6.87 (d, 1H, J = 8.3 Hz), 6.46–6.57 (m, 4H), 4.63 (s, 2H), 3.88 (s, 3H), 3.84 (s, 3H), 3.72 (s, 6H), 2.35 (s, 3H), 2.36 (s, 3H); MS (ESI): *m/z* 535 [M+1]$^+$; HRMS (ESI *m/z*) [M+1]$^+$ calcd for $C_{29}H_{30}N_2O_6S$: 535.1569, found: 535.1578.

*4.17. (Z)-2-(2-methoxy-5-(3,4,5-trimethoxystyryl)phenoxy)-N-(benzo[d]thiazol-6-yl) acetamide (**12a**)*

This compound was prepared according to the method described for compound **11a** by employing (Z)-2-(2-methoxy-5-(3,4,5-trimethoxystyryl) phenoxy)acetic acid (**10**) (374 mg, 1.0 mmol), and 6-aminobenzothiazole (150 mg, 1.0 mmol) to obtain the pure product **12a** (451 mg, 89% yield) as white solid; mp: 111–114 °C; ^{1}H NMR (200 MHz, $CDCl_3$): δ = 9.19 (br s, 1H), 9.15 (s, 1H), 8.69 (d, 1H, J = 2.4 Hz), 8.24 (d, 1H, J = 8.1 Hz), 7.34–7.37 (dd, 1H, J = 8.9, 2.4 Hz), 6.97–7.02 (dd, 1H, J = 8.1, 1.6 Hz), 6.92 (d, 1H, J = 2.4 Hz), 6.84 (d, 1H, J = 8.1 Hz), 6.5 (d, 1H, J = 12.2 Hz), 6.44–6.48 (m, 3H), 4.53 (s, 2H), 3.95 (s, 3H), 3.84 (s, 3H), 3.68 (s, 6H); ^{13}C NMR (75 MHz, $CDCl_3$): δ = 166.99, 156.49, 153.01, 148.84, 148.04, 146.71, 135.58, 134.46, 132.51, 130.70, 129.81, 128.67, 124.65, 123.17, 119.51, 117.54, 112.39, 111.83, 105.86, 70.41, 60.95, 56.13, 55.93; MS (ESI): *m/z* 507 [M+1]$^+$; HRMS (ESI *m/z*) [M+1]$^+$ calcd for $C_{27}H_{27}N_2O_6S$: 507.2369, found: 507.2345.

*4.18. (Z)-2-(2-methoxy-5-(3,4,5-trimethoxystyryl)phenoxy)-N-(2-methylbenzo[d]thiazol-6-yl) acetamide (**12b**)*

This compound was prepared according to the method described for compound **11a** by employing (Z)-2-(2-methoxy-5-(3,4,5-trimethoxystyryl) phenoxy)acetic acid (**10**) (374 mg, 1.0 mmol) and 6-amino-2-methylbenzothiazole (164 mg, 1.0 mmol) to obtain the pure product **12b** (460 mg, 88% yield); mp: 112–114 °C; ^{1}H NMR (300 MHz, $CDCl_3$): δ = 9.24 (s, 1H), 8.2 (d, 1H, J = 1.7 Hz), 7.79 (d, 1H, J = 8.9 Hz), 7.62–7.67 (dd, 1H, J = 8.9, 1.7 Hz), 6.98–7.03 (dd, 1H, J = 8.9, 1.7 Hz), 6.95 (d, 1H, J = 1.7 Hz), 6.87 (d, 1H, J = 8.9 Hz), 6.44–6.54 (m, 4H), 4.54 (s, 2H), 3.95 (s, 3H), 3.82 (s, 3H), 3.69 (s, 6H), 2.85 (s, 3H); ^{13}C NMR (300 MHz, $CDCl_3$): δ = 167.48, 166.10, 153.13, 152.23, 148.33, 146.41, 136.45, 135.61, 131.95, 130.34, 129.70, 128.85, 128.43, 123.36, 120.89, 117.13, 116.34, 112.64, 111.37, 105.40, 69.39, 60.02, 55.46, 55.24, 19.55; IR (KBr) (ν_{max}/cm^{-1}): 3388, 2936, 1690, 1576, 1518, 1464, 1431, 1416, 1325, 1251, 1124, 1057, 1003, 882, 803, 777; MS (ESI): *m/z* 521 [M+1]$^+$; HRMS (ESI *m/z*) [M+1]$^+$ calcd for $C_{28}H_{29}N_2O_6S$: 521.1746, found: 521.1733.

5. Materials and methods

5.1. Cell culture

MCF-7 cells (human breast cancer) were incubated by using Dulbecco's modified Eagle's medium (DMEM), supplemented with 10% fetal calf serum, 100 μg/mL pencillin-G and 100 μg/mL streptomycin sulfate (Sigma). The cell lines were maintained at 37 °C in a humidified atmosphere containing 5% CO_2 in the incubator.

5.2. In vitro anticancer evaluation

All the synthesized compounds were evaluated for their *in vitro* anticancer activity in different cancer cell lines by using sulforhodamine B (SRB) protein assay in 96 well plate under 10% fetal bovine serum at 37 °C, 5% CO_2, and 100% relative humidity in DMEM medium. Cancer cells were seeded in 96 well plate and drugs of 10 μM concentration were added after 24 h of incubation. The treated cells were incubated for 48 h and then cells were processed according to the standard protocol. The absorbance was read on an ELISA plate reader at a wavelength of 560 nm. Growth percentage was calculated for test wells relative to control wells.

5.3. Cell viability

Cell viability was assessed by the MTT based assay. MCF-7 cells were seeded in a 96-well plate (TPP) at a cell density of 10,000 cells/well. After overnight incubation, the cells were treated with compounds CA-4, BT, **11a**, **11b**, **11e**, **11f**, **11g**, **11h**, **11i**, **11j**, **11k** and **12b** and were incubated for 24 h. The medium was then discarded and replaced with fresh 100 μL media followed by addition of 10 μL of MTT dye. Plates were incubated at 37 °C for 2 h. The absorbance (O.D) was measured at 570 nm using Multimode Varioskan Flash (Thermo Fisher Scientifics).

5.4. Cell cycle analysis

5×10^5cells each of MCF-7 seeded in 60 mm dish and were allowed to grow for 24 h. A concentration of 4 μM of CA-4, BT, **11a**, **11b**, **11e**, **11f**, **11g**, **11h**, **11i**, **11j**, **11k** and **12b** was added to the culture media, and the cells were incubated for an additional 24 h. Cells were harvested with Trypsin-EDTA, fixed with ice-cold 70% ethanol at 4 °C for 30 min, washed with PBS and incubated with 1 mg/ml RNaseA solution (Sigma) at 37 °C for 30 min. Cells were collected by centrifugation at 2000 rpm for 5 min and further stained with 250 μL of DNA staining solution [10 mg of propidium iodide (PI), 0.1 mg of trisodium citrate, and 0.03 mL of Triton X-100 were dissolved in 100 mL of sterile MilliQ water at room temperature for 30 min in the dark]. The DNA contents of 20,000 events were measured by flow cytometer (DAKO CYTOMATION, Beckman Coulter, Brea, CA). Histograms were analyzed using Summit Software.

5.5. Tubulin polymerization assay

Tubulin polymerization assay was conducted with cytoskeleton kit (BK-004). The compounds **11a**, CA-4, nocadazole, paclitaxel was incubated with tubulin (100 μl) that was provided in the kit and the readings were taken for 30 min to 1 h. The O.D at 340 nm was taken and inhibition graph was plotted.

5.6. Protein extraction and Western blot analysis

Total cell lysates from cultured MCF-7cells were obtained by lysing the cells in ice-cold RIPA buffer (1xPBS, 1% NP-40, 0.5% sodium deoxycholate and 0.1% SDS) and containing 100 μg/mL PMSF, 5 μg/mL Aprotinin, 5 μg/mL leupeptin, 5 μg/mL pepstatin and 100 μg/mL NaF. After centrifugation at 12,000 rpm for 10 min, the protein in supernatant was quantified by Bradford method (BIO-RAD) using Multimode varioskan instrument (Thermo-Fischer Scientifics). Fifty micrograms of protein per lane was applied in 12% SDS-polyacrylamide gel. After electrophoresis, the protein was transferred to polyvinylidine difluoride (PVDF) membrane (Amersham Biosciences). The membrane was blocked at room temperature for 2 h in TBS + 0.1% Tween20 (TBST) containing 5% blocking powder (Santacruz). The membrane was washed with TBST for 5 min, and primary antibody was added and incubated at 4 °C overnight (O/N). Antibodies like *c*-Jun, ERK and phosphorylated form of ERK were purchased from Cell Signalling technology, USA. The membrane was incubated with corresponding horseradish peroxidase-labeled secondary antibody (1:2000) (Santa Cruz) at room temperature for 1 h. Membranes were washed with TBST three times for 15 min and the blots were visualized with chemiluminescence reagent (Thermo Fischer Scientifics Ltd.). The X-ray films were developed with developer and fixed with fixer solution.

5.7. Immunofluorescence

Human breast cancer (MCF-7) cells were seeded on cover slips and treated with compounds at concentration of 4 μM for 24 h. After treatment, cover slips were fixed with a paraformaldehyde solution (4% in 1× PBS) for 20 min at room temperature. Cell permeabilization was achieved by administration of a Triton X-100 solution (0.2% in 1× PBS) for 5min. Then cover slips were kept in 100% methanol at 4 °C overnight. Subsequently, cover slips were blocked with a 1% BSA solution for 60 min and then incubated with anti-ERK phosphorylated antibody (or) α-tubulin antibody (1:100) at room temperature for 2 h. The slides were washed three times each of 5 min with PBST. Then cover slips were incubated with a FITC-conjugated anti-rabbit secondary antibody (Jackson Immuno Research Laboratories Inc., Pennsylvania, USA) for 1 h and cover slips were washed three times with PBST solution and mounted with DAPI/PI solution. Finally, cells were observed under confocal microscope (Olympus FV1000). Images taken were processed with the support of the flow view version 1.7c software program.

5.8. Docking

ERK2 with small molecule inhibitor (PDB code: 1TVO) and Tubilin bound with colchicine (PDB code: 3E22) was selected as the receptor for docking simulation. Ligand bound in the ATP binding site and colchicine pocket nearby solvent molecules were removed followed by addition of hydrogen atoms to the entire protein. Coordinates for each compound in the current study were obtained using Chemdraw11 followed by MM2 energy minimization. Docking was carried out by AutoDock4 [54] in the ATP-binding pocket of ERK2. Grid map in Autodock that defines the interaction of protein and ligands in binding pocket was defined. The grid map was used with 60 points in each *x*, *y* and *z* direction, equally spaced at 0.375 Å. Docking was performed using the Lamarckian genetic algorithm in AutoDock4 [55]. Each docking experiment was performed 10 times, yielding 10 docked conformations. Parameters used for the docking were as follows: population size of 150; random starting position and conformation; maximal mutation of 2 Å in translation and 50° in rotations; elitism of 1; mutation rate of 0.02 and crossover rate of 0.8; and local search rate of 0.06. Simulations were performed with a maximum of 1.5 million energy evaluations and a maximum of 27,000 generations. Final docked conformations were clustered

using a tolerance of 1.0 Å root mean square deviation (RMSD). The best model was picked based on the best stabilization energy.

5.9. Molecular dynamics

The most stable structure of ERK2-inhibitor complexes obtained from docking simulation were equilibrated in solution through 1.0 ns MD simulation with Gromacs-4.5.5 [56]. Topology files consistent with this force field were generated for each inhibitor using the PRODRG server and modified the partial atomic charges according to GROMOS96 force field. The equilibration procedure started with addition of chlorine ions as the counter ion to neutralize the total charge of all atom of ERK2. Prior to energy minimization, the inhibitor-ERK2 complexes were immersed in a box of flexible SPC water molecules [57] such that the minimum distance of any non-water atom to the edge of the box was 4.0 Å; typical calculations included ~10,000 water molecules. After 1000 cycle of energy minimization to remove bad Van der Waals contacts, we equilibrated the system beginning with 100 ps equilibration dynamics of solvent molecules at 300 K. The next step involved equilibration of solute at 100-ps pressure. Then, the equilibration dynamics of the entire system was performed at 1 ns using periodic boundary condition.

Acknowledgments

The author A.M.R is thankful to CSIR, India and, P.S. & C.K. are thankful to UGC, India for the award of research fellowships.

References

[1] M.H. Cobb, E.J. Goldsmith, J. Biol. Chem. 270 (1995) 14843–14846.
[2] R. Seger, E.G. Krebs, FASEB J. 9 (1995) 726–735.
[3] T.S. Lewis, P.S. Shapiro, N.G. Ahn, Adv. Cancer Res. 74 (1998) 49–139.
[4] G. Pearson, F. Robinson, T.B. Gibson, B.-E. Xu, M. Karandikar, K. Berman, M.H. Cobb, Endocr. Rev. 22 (2001) 153–183.
[5] M. Yamada, T. Ikeuchi, H. Hatanaka, Prog. Neurobiol. 51 (1997) 193–197.
[6] K. Hickey, D. Grehan, I.M. Reid, S. O'Brian, T.N. Walsh, T.P.J. Hennessy, Cancer 74 (1994) 1693–1698.
[7] H. Chen, G. Zhu, Y. Li, R.N. Padia, Z. Dong, Z.K. Pan, K. Liu, S. Huang, Cancer Res. 69 (2009) 9228–9235.
[8] G.R. Pettit, S.B. Singh, E. Hamel, C.M. Lin, D.S. Alberts, D. Garcia-Kendall, Experientia 45 (1989) 209–211.
[9] G.M. Cragg, D.G. Kingston, D.J. Newman, Boca Raton, FL, 2005.
[10] M.M. Cooney, J. Ortiz, R.M. Bukowski, S.C. Remick, Curr. Oncol. Rep. 7 (2005) 90–95.
[11] S.L. Young, D.J. Chaplin, Expert. Opin. Invest. Drugs 13 (2004) 1171–1182.
[12] http://www.clinicaltrials.gov/ct/gui/show/NCT00060242.
[13] G.J. Rustin, G. Shreeves, P.D. Nathan, A. Gaya, T.S. Ganesan, D. Wang, J. Boxall, L. Poupard, D.J. Chaplin, M.R. Stratford, J. Balkissoon, M.A. Zweifel, Br. J. Cancer 102 (2010) 1355–1360.
[14] G.R. Pettit, M.R. Rhodes, D.L. Herald, E. Hamel, J.M. Schmidt, R.K. Pettit, J. Med. Chem. 48 (2005) 4087–4099.
[15] G.C. Tron, T. Pirali, G. Sorba, F. Pagliai, S. Busacca, A. Genazzani, J. Med. Chem. 49 (2006) 3033–3044.
[16] N.H. Nam, Curr. Med. Chem. 10 (2003) 1697–1722.
[17] J.P. Liou, Y.L. Chang, F.M. Kuo, C.W. Chang, H.Y. Tseng, C.C. Wang, Y.N. Yang, J.Y. Chang, S.J. Lee, H.P. Hsieh, J. Med. Chem. 47 (2004) 4247–4257.
[18] K. Ohsumi, R. Nakagawa, Y. Fukuda, T. Hatanaka, Y. Morinaga, Y. Nihei, K. Ohishi, Y. Suga, Y. Akiyama, T. Tsuji, J. Med. Chem. 41 (1998) 3022–3032.
[19] P. Hinnen, F.A.L.M. Eskens, Br. J. Cancer 96 (2007) 1159–1165.
[20] M. Cushman, H.M. He, C.M. Lin, E. Hamel, J. Med. Chem. 36 (1993) 2817–2821.
[21] J.A. Hadfield, S. Ducki, N. Hirst, A.T. McGown, Prog. Cell Cycle Res. 5 (2003) 309–325.
[22] C. Kanthou, G.M. Tozer, Int. J. Exp. Pathol. 90 (2009) 284–294.
[23] J.W. Lippert, Bioorg. Med. Chem. 15 (2007) 605–615.
[24] K.G. Pinney, M.P. Mejia, V.M. Villalobos, B.E. Rosenquist, G.R. Pettit, P. Verdier-Pinard, E. Hamel, Bioorg. Med. Chem. 8 (2000) 2417–2425.
[25] H. Quan, Y. Xu, L. Lou, Int. J. Cancer 122 (2008) 1730–1737.
[26] J. Mizoule, B. Meldrum, M. Mazadier, M. Croucher, C. Ollat, A. Uzan, J.J. Legrand, C. Gueremy, C.G. Le Fur, Neuropharmacology 24 (1985) 767–773.
[27] T. Tanaka, H. Umekawa, M. Saitoh, T. Ishikawa, T. Shin, M. Ito, H. Itoh, Y. Kawamatsu, H. Sugihara, H. Hidaka, Mol. Pharmacol. 29 (1986) 264–269.
[28] T.D. Bradshaw, S. Wrigley, D.-F. Shi, R.J. Schultz, K.D. Paull, M.F.G. Stevens, Br. J. Cancer 77 (1998) 745–752.
[29] I. Hutchinson, S.A. Jennings, B.R. Vishnuvajjala, A.D. Westwell, M.F.G. Stevens, J. Med. Chem. 45 (2002) 744–747.
[30] V. Beneteau, T. Besson, J. Guillard, S. Leonce, B. Pfeiffer, Eur. J. Med. Chem. 34 (1999) 1053–1060.
[31] E.T. Kisak, B. Coldren, C.A. Evans, C. Boyer, J.A. Zasadzinski, Curr. Med. Chem. 11 (2004) 1241–1253.
[32] S.H.L. Kok, R. Gambari, C.H. Chui, M.C.W. Yuen, E. Lin, R.S.M. Wong, F.Y. Lau, G.Y.M. Cheng, W.S. Lam, S.H. Chan, K.H. Lam, C.H. Cheng, P.B.S. Lai, M.W.Y. Yu, F. Cheung, J.C.O. Tanga, A.S.C. Chana, Bioorg. Med. Chem. 16 (2008) 3626–3631.
[33] B.A. Song, X.H. Liu, S. Yang, D.Y. Hu, L.H. Gin, H. Zhang, Chin. J. Chem. 23 (2005) 1236–1240.
[34] G.R. Pettit, S.B. Singh, M.R. Boyd, E. Hamel, R.K. Pettit, J.M. Schmidt, F. Hogan, J. Med. Chem. 38 (1995) 1666–1672.
[35] G.R. Pettit, S.B. Singh, G.M. Cragg, J. Org. Chem. 50 (1985) 3404–3406.
[36] A. Kamal, Y.V.V. Srikanth, T.B. Shaik, M.N.A. Khan, Md. Ashraf, M.K. Reddy, K.A. Kumar, S.V. Kalivendi, Med. Chem. Commun. 12 (2011) 819–823.
[37] http://dtp.nci.nih.gov/branches/btb/ivclsp.html.
[38] (a) A. Kamal, G.R. Krishna, P. Raju, A. Viswanath, M.J. Ramaiah, G.B. Kishan, M.P. Bhadra, Bioorg. Med. Chem. Lett. 20 (2010) 4865–4869;
(b) V. Trapani, V. Patel, C.O. Leong, H.P. Ciolino, G.C. Yeh, C. Hose, J.B. Trepel, M.F.G. Stevens, E.A. Sausville, A.I. Loaiza-Perez, Br. J. Cancer 88 (2003) 599–605.
[39] C. Kanthou, O. Greco, A. Stanford, I. Cook, R. Knight, O. Benzakour, G. Tozer, Am. J. Pathol. 165 (2004) 1401–1411.
[40] A.A. Reszka, R. Seger, C.D. Diltz, E.G. Krebs, E.H. Fischer, Proc. Natl. Acad. Sci. U.S.A. 92 (1995) 8881–8885.
[41] M.M. Kawahima, K. Kosik, Mol. Biol. Cell. 7 (1996) 893–905.
[42] A. Ding, B. Chen, M. Fuortes, E. Blum, J. Exp. Med. 183 (1996) 1899–1904.
[43] M.H. Verlhac, H. dePennart, B. Maro, M.H. Cobb, H.J. Clarke, Dev. Biol. 158 (1993) 330–340.
[44] P.S. Shapiro, E. Vaisberg, A.J. Hunt, N.S. Tolwinski, A.M. Whalen, J.R. McIntosh, N.G. Ahn, J. Cell. Biol. 142 (1998) 1533–1545.
[45] J.H. Wright, E. Munar, D.R. Jameson, P.R. Andreassen, R.L. Margolis, Proc. Natl. Acad. Sci. U.S.A. 96 (1999) 11335–11340.
[46] C. Hayne, G. Tzivion, Z. Luo, J. Biol. Chem. 275 (2000) 31876–31882.
[47] W.F. Tan, X.W. Zhang, M.H. Li, J.M. Yue, Y. Chen, L.P. Lin, Eur. J. Pharmacol. 499 (2004) 219–228.
[48] J.A. Gollob, S. Wilhelm, C. Carter, S.L. Kelley, Semin. Oncol. 33 (2006) 392–406.
[49] S. Tanimura, A. Uchiyama, K. Watanabe, M. Yasunaga, Y. Inada, T. Kawabata, K. Iwashita, S. Noda, K. Ozaki, M. Kohno, Biochem. Biophys. Res. Commun. 378 (2009) 650–655.
[50] M.M. Vleugel, A.E. Greijer, R. Bos, E. Vanderwall, P.J. VanDiest, Hum. Pathol. 37 (2006) 668–674.
[51] G.L. Johnson, R. Lapadat, Science 298 (2002) 1911–1912.
[52] J.L. Yap, S. Worlikar, A.D. Mackerell Jr., P. Shapiro, S. Fletcher, Chem. Med. Chem. 6 (2011) 38–48.
[53] Y. Zhang, X. Pu, M. Shi, L. Chen, Y. Song, L. Qian, G. Yuan, H. Zhang, M. Yu, M. Hu, B. Shen, N. Guo, BMC Cancer 7 (2007) 145.
[54] AutoDock, version 4.0: http://www.scripps.edu/mb/olson/doc/autodock/.
[55] G.M. Morris, D.S. Goodsell, R.S. Halliday, R. Huey, W.E. Hart, R.K. Belew, A.J. Olson, J. Comput. Chem. 19 (1998) 1639–1662.
[56] B. Hess, C. Kutzner, D.V. Spoel, E. Lindahl, GROMACS 4: Algorithms for highly efficient, load-balanced, and scalable molecular simulation.
[57] H.J.C. Berendsen, J.P.M. Postman, W.F.V. Gunsteren, J. Hermans, in: B. Pullman (Ed.), Interaction Models for Water in Relation to Protein Hydration, Reidel Publishing Co., Dordrecht, The Netherlands, 1981, p. 331.